

# Generating long sequences of high-intensity femtosecond pulses

M. Bitter and V. Milner

*Department of Physics & Astronomy and The Laboratory for Advanced Spectroscopy and Imaging Research (LASIR),  
The University of British Columbia, Vancouver, Canada*

(Dated: April 24, 2022)

We present an approach to create pulse sequences extending beyond 150 picoseconds in duration, comprised of 100  $\mu\text{J}$  femtosecond pulses. A quarter of the pulse train is produced by a high-resolution pulse shaper, which allows full controllability over the timing of each pulse. Two nested Michelson interferometers follow to quadruple the pulse number and the sequence duration. To boost the pulse energy, the long train is sent through a multi-pass Ti:Sapphire amplifier, followed by an external compressor. A periodic sequence of 84 pulses of 120 fs width and an average pulse energy of 107  $\mu\text{J}$ , separated by 2 ps, is demonstrated as a proof of principle.

## I. INTRODUCTION

Series of ultrashort laser pulses, also known as *pulse trains* (PT), have found widespread use in the field of quantum coherent control of matter with laser light (for a recent review of this topic, see [1] and references therein). Numerous applications require multiple pulses of relatively high intensity, on the order of  $10^{13}$  to  $10^{14}$   $\text{W}/\text{cm}^2$ , to attain the regime of strong-field interaction with each pulse, just below the damage threshold of the material system under study. Using coherent control of molecular rotation - an area of our own expertise - as only one representative example: Sequences of intense ultrashort pulses have been key in enhancing molecular alignment [2–4] and aligning asymmetric top molecules in three dimensions [5, 6], selective excitation of molecular isotopes and spin isomers [7, 8], initiating uni-directional rotation [9–11] and controlling gas hydrodynamics [12], as well as studying the quantum  $\delta$ -kicked rotor in a series of recent fundamental works [13–16]. The great utility of PTs stems from two main factors. First, by matching the timing of pulses in the train to the dynamics of the system of interest, e.g. the vibrational or rotational period of a molecule, one can often significantly improve the selectivity of excitation. Second, the ability to re-distribute the energy among multiple pulses without losing the cumulative excitation strength enables one to avoid detrimental strong-field effects, such as molecular ionization and gas filamentation.

There are two common techniques to produce a pulse train with variable time separation between transform-limited pulses. In the first technique, the incoming laser pulse is split into  $2^n$  pulses using  $n$  nested Michelson interferometers (MI). Even though sequences of up to 16 pulses [17] have been generated using this method, the scheme becomes increasingly more difficult to implement with the increasing value of  $n$ . We also note, that the control over the pulse timing is rather limited in that it cannot be changed independently for each individual pulse in the train. Similarly limited flexibility is characteristic of a pulse splitting method based on stacking a number of birefringent crystals [18].

The second common approach is based on the tech-

nique of femtosecond pulse shaping (PS) where the spatially dispersed frequency components of the pulse are controlled in phase and amplitude [19, 20], or via the direct space-to-time conversion [21]. This offers much higher flexibility at the expense of being limited to the relatively low energy trains. The latter limitation is due to both the damage threshold of a typical pulse shaper, and also the necessity to block multiple spectral components in order to generate a train of pulses in the time domain. Phase-only shaping has been often used to create a series of pulses without the loss of energy [22], but in this case, the distribution of the pulse amplitudes within the train is uneven and no control over this distribution is available.

Here we report on the generation of femtosecond pulse trains, that simultaneously satisfy the following specific characteristics: (1) consist of a large number of transform-limited pulses; (2) exhibit a relatively flat amplitude envelope; (3) can be easily tuned in terms of the timing of the constituent pulses; and (4) carry energies in excess of 100  $\mu\text{J}$  per pulse. Our method is based on the combination of a pulse shaper, which provides the often required flexibility in controlling the timing and amplitudes of individual pulses on the time scale of 50 ps, and a set of nested Michelson interferometers, which enables extending the overall length of the train to much longer times. Key to our approach is the integration of a multi-pass amplifier (MPA), which compensates the energy loss during the pulse shaping stage. We note that although amplification of shaped pulses is commonly used in chirped-pulse amplifiers [23, 24], and has also been employed to amplify pulse sequences [20, 25–27], to our knowledge, pulse trains with the above mentioned specifications have not been demonstrated. We discuss the versatility of the developed tool and demonstrate an example of a long pulse train consisting of 84 equally strong pulses.

## II. EXPERIMENTAL SETUP

We start with a Ti:Sapphire femtosecond laser system (SpitFire Pro, Spectra-Physics) producing uncom-

pressed frequency-chirped pulses with the spectral bandwidth of 9 nm (full width at half maximum) at the central wavelength of 800 nm, 1 KHz repetition rate and 2 mJ per pulse. Part of the beam (60% in energy) is compressed to 120 fs pulses (full width at half maximum) via a grating compressor and is used as a reference in cross-correlation measurements. The second part is sent to a femtosecond pulse shaper which splits a single chirped pulse into a series of pulses, as schematically shown in Fig.1. The shaper is built in the standard  $4f$ -geometry [28] and uses a liquid crystal spatial light modulator (SLM, Cambridge Research and Instrumentation, Inc.) with a double-layer 640-pixel mask. We control the spectral phase and amplitude of the laser pulse to achieve the desired waveform of the output train. The required frequency masks are calculated through the Fourier transform of the target temporal profile (for more details see Ref. [28]). The spectral resolution of  $\Delta\lambda = 0.04\text{nm}$  per pixel sets the upper limit for the total duration of the pulse train to  $T = \lambda^2/c\Delta\lambda \approx 50\text{ps}$ , where the central wavelength  $\lambda = 800\text{nm}$  and  $c$  is the speed of light in vacuum. The shaper is followed by two nested Michelson interferometers, shown inside the dotted box in Fig.1. In contrast to the pulse shaper, the interferometric setup has no limitation on the overall length of the final pulse train. It allows to quadruple the number of pulses in the sequence and extend its duration to at least four times that produced by the shaper.

Unavoidable optical energy losses in the combined PS+MI setup can be quantified as follows. About 50% of energy is lost in a typical  $4f$  pulse shaper due to the diffraction efficiency of the gratings. The energy throughput owing to the splitting of the initial pulse into a sequence of  $N$  identical pulses by means of the spectral shaping can be estimated as  $1/N$  [29]. Another factor of  $1/2$  accounts for the polarization multiplexing in the MI setup. In total, each of the  $4N$  pulses in the train carries  $1/(16N^2)$  of the available input energy. Since the latter is typically limited to about 1 mJ by the damage threshold of a pulse shaper (300  $\mu\text{J}$  in our case), for a train of  $4N = 84$  pulses demonstrated in this work, one ends up with  $\lesssim 0.2 \mu\text{J}$  per pulse. Imperfections of various optical components bring this number even further down, well below the typical requirements for a strong-field regime of the laser-molecule interaction.

To compensate for the energy losses described above, we send the long pulse train through a home-built multi-pass amplifier, schematically shown inside the dashed box in Fig. 1. After passing four times through a Ti:Sapphire crystal, pumped by a Neodymium YAG laser (Powerlite Precision II, Continuum, 800 mJ at 532 nm and 10 Hz repetition rate), the pulses are amplified by a factor of up to 2800, reaching the energy of more than 100  $\mu\text{J}$  per pulse. Both the pulse shaping and the interferometric splitting are applied to uncompressed frequency-chirped 150 ps pulses, so as to lower the peak intensities of the amplified pulses inside the MPA below the damage threshold of the Ti:Sapphire crystal. Chirped am-

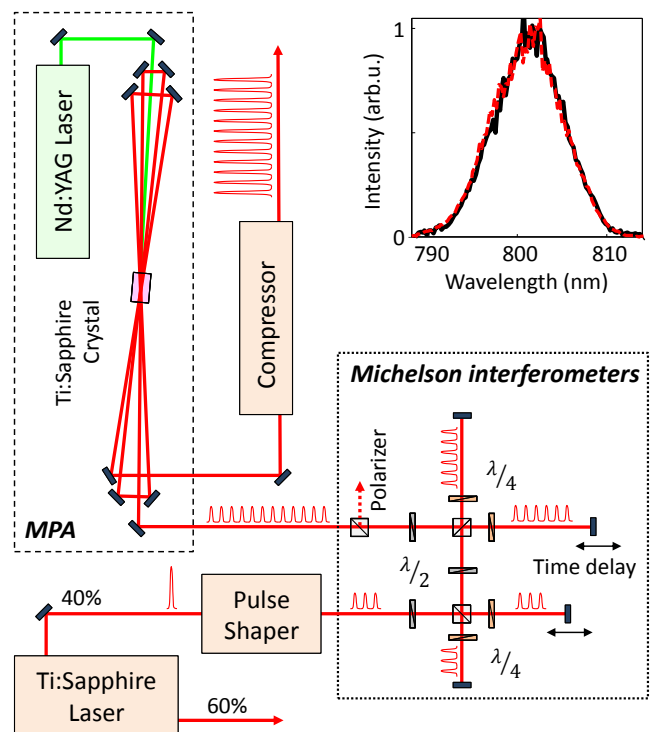


FIG. 1: (color online) Optical setup for the generation of long sequences of high-energy femtosecond pulses. See text for details. Inset: Spectrum of a single pulse before (black solid, 0.4  $\mu\text{J}$ ) and after (red dashed, 100  $\mu\text{J}$ ) the amplification in the multi-pass amplifier (MPA).

plification also ensures negligible spectral distortions of the output pulses, as demonstrated in the inset of Fig. 1. The spectrum of a single pulse amplified 250 times to an energy of 100  $\mu\text{J}$  (red dashed line) is almost indistinguishable from the spectrum of an unamplified pulse at 0.4  $\mu\text{J}$  (black solid line). The MPA is followed by a standard grating-based pulse compressor that compresses each pulse of the sequence to a 120 fs duration.

### III. AMPLIFIED PULSE SEQUENCES

First, we discuss pulse sequences which can be created with the pulse shaper only, i.e. without the use of Michelson interferometers. The pulse trains are characterized using the technique of cross-correlation frequency-resolved optical gating (xFROG) with a well-known transform-limited reference pulse. Figure 2(a) shows an xFROG spectrogram for the pulse train of 21 equally spaced pulses with a period of 2 ps. The spectrogram demonstrates that each pulse in the train is transform-limited with no residual frequency chirp, confirming that proper pulse compression is attainable at the end of the combined shaping and amplification processes.

Integrating over the whole spectrum, one finds the distribution of energy among the pulses in the train, plotted in Fig. 2(b). Here, the gain factor of 400 was required

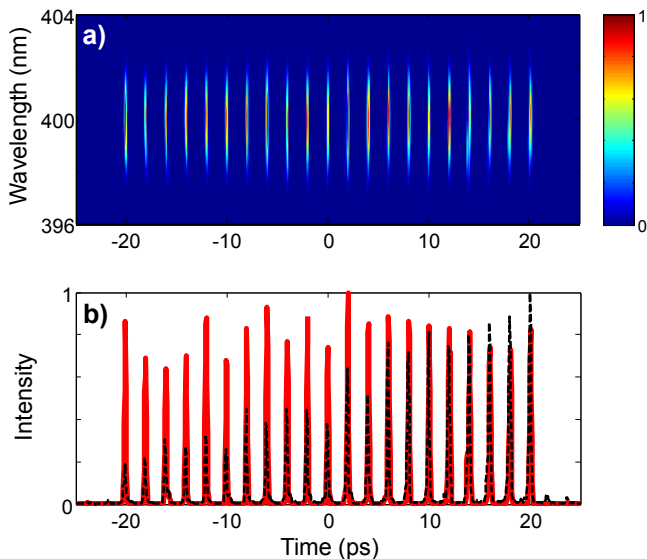


FIG. 2: (color online) (a) xFROG spectrogram of an amplified pulse train with 21 equally spaced pulses and (b) its corresponding temporal profile before (dashed black) and after (solid red) the MPA amplification by a factor of 400.

for reaching an average energy of  $124 \mu\text{J}$  per pulse. Such high gain levels result in the increased sensitivity of the output pulse sequence to the energy fluctuations in the seed train entering the MPA, as well as in pulse dependent amplification rates. Equalizing the output amplitudes is achieved through the iterative process, in which the correction function is fed back to the pulse shaper in order to compensate for the irregularities in the output temporal profile. In the presented example, the corrected seed train is shown in Fig. 2(b) by the black dashed line. The final degree of flatness is limited by the nonlinearity of the MPA amplification process and is on the order of 10%, determined as the standard deviation of the pulse-to-pulse energy fluctuations.

Femtosecond pulse shaping offers the flexibility of creating arbitrary pulse sequences within the limits of the shaper's temporal and spectral resolution. In Fig. 3, we demonstrate this flexibility using the example of a pulse train with nine pulses. The overall energy of the train was set to 1 mJ. A flat train of pulses with almost equal amplitudes (7% flatness) separated by  $T = 4\text{ps}$  is shown in Fig. 3(a). In Fig. 3(b), a linear amplitude tilt was applied to the train's envelope and its sixth pulse was completely suppressed, while the total energy was kept constant at 1 mJ. Figures 3(c) and (d) demonstrate our ability to produce high-energy flat-amplitude sequences with multiple periods and completely random timing of pulses, respectively.

Adding a set of nested Michelson interferometers enables us to generate pulse sequences longer than the time limit set by the spectral resolution of the shaper (in our case, 50 ps) and with more pulses, while still maintaining the energy level in excess of  $100 \mu\text{J}$  per pulse. In Figures 4(a) and (b), we show periodic sequences of 20 and

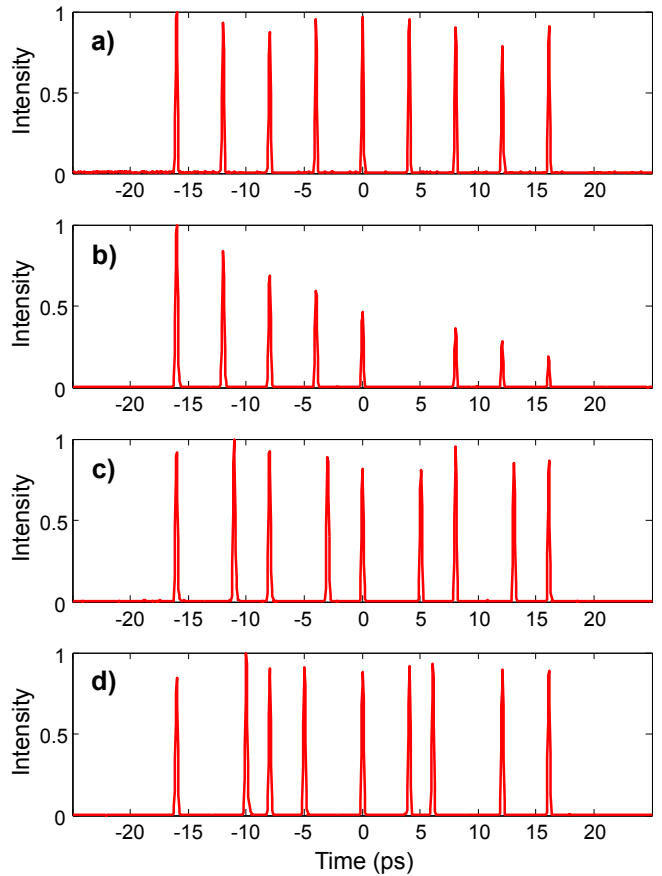


FIG. 3: Temporal profiles of four different sequences of nine pulses: (a) Periodic train of equal-amplitude pulses separated by 4 ps. (b) Same train with linearly decreasing pulse amplitudes and the sixth pulse suppressed. (c) Flat pulse train with two different time periods of 5 ps and 3 ps. (d) Flat non-periodic pulse sequence with a random timing of pulses.

84 pulses stretching over a duration of  $\approx 170$  ps (pulse separation of 8 ps and 2 ps, respectively) and carrying  $\approx 110\mu\text{J}$  per pulse. The latter train has been amplified 2800 times to the total energy of 9 mJ. One can see that longer pulse trains suffer from a higher amplitude noise, e.g. standard deviations of 13% and 18% in Fig.4(a) and (b), respectively. The increasing noise is due to the higher MPA amplification factors and the correspondingly higher nonlinearity of the amplification process.

#### IV. SUMMARY

We implemented an optical setup that produces long sequences of femtosecond pulses. The setup is based on the combination of femtosecond pulse shaping, interferometric pulse splitting and multi-pass amplification. The shaping offers the flexibility of creating arbitrary pulse trains on the time scale of 50 ps. The duration of the train can be further increased (in this work, fourfold) by means of the setup of nested Michelson interferometers. Finally, multi-pass amplification compensates for the se-

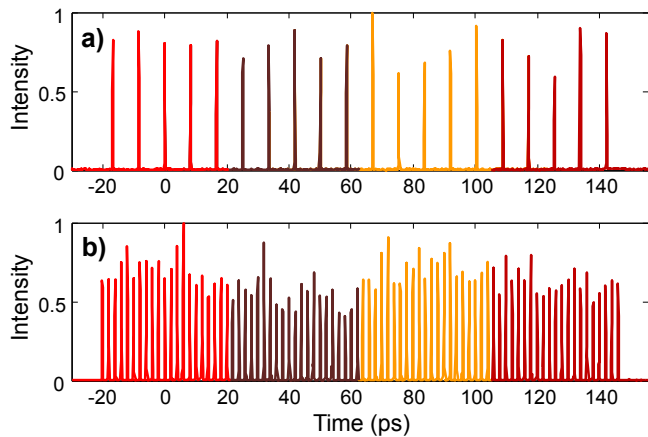


FIG. 4: (color online) Temporal profile of two periodic pulse sequences: (a) 20 pulses separated by 8 ps and amplified 500 times to  $114 \mu\text{J}$  per pulse; (b) 84 pulses separated by 2 ps and amplified 2800 times to  $107 \mu\text{J}$  per pulse. The four colors represent the four different pathways through the Michelson interferometers.

vere energy losses typically associated with the generation of long pulse sequences from a single femtosecond pulse. An example of a train of 84 pulses separated by 2 ps with an energy exceeding  $100 \mu\text{J}$  per 120 fs pulse is presented.

We are grateful to Jonathan Morrison and Kamil Krawczyk for their help with the optical setup.

- 
- [1] J. Voll and R. d. Vivie-Riedle, “Pulse trains in molecular dynamics and coherent spectroscopy: a theoretical study,” *New J. Phys.* **11**, 105036 (2009).
- [2] C. Z. Bisgaard, M. D. Poulsen, E. Peronne, S. S. Viftrup, and H. Stapelfeldt, “Observation of enhanced field-free molecular alignment by two laser pulses,” *Phys. Rev. Lett.* **92**, 173004 (2004).
- [3] K. F. Lee, I. V. Litvinyuk, P. W. Dooley, M. Spanner, D. M. Villeneuve, and P. B. Corkum, “Two-pulse alignment of molecules,” *J. Phys. B* **37**, L43 (2004).
- [4] J. P. Cryan, P. H. Bucksbaum, and R. N. Coffee, “Field-free alignment in repetitively kicked nitrogen gas,” *Phys. Rev. A* **80**, 063412 (2009).
- [5] K. F. Lee, D. M. Villeneuve, P. B. Corkum, A. Stolow, and J. G. Underwood, “Field-free three-dimensional alignment of polyatomic molecules,” *Phys. Rev. Lett.* **97**, 173001 (2006).
- [6] X. Ren, V. Makhija, and V. Kumarappan, “Multi-pulse three-dimensional alignment of asymmetric top molecules,” *Phys. Rev. Lett.* **112**, 173602 (2014).
- [7] S. Fleischer, I. Sh. Averbukh, and Y. Prior, “Isotope-selective laser molecular alignment,” *Phys. Rev. A* **74**, 041403–4 (2006).
- [8] S. Fleischer, I. Sh. Averbukh, and Y. Prior, “Selective alignment of molecular spin isomers,” *Phys. Rev. Lett.* **99**, 093002 (2007).
- [9] S. Fleischer, Y. Khodorkovsky, Y. Prior, and I. Sh. Averbukh, “Controlling the sense of molecular rotation,” *New J. Phys.* **11**, 105039 (2009).
- [10] K. Kitano, H. Hasegawa, and Y. Ohshima, “Ultrafast angular momentum orientation by linearly polarized laser fields,” *Phys. Rev. Lett.* **103**, 223002 (2009).
- [11] S. Zhdanovich, A. A. Milner, C. Bloomquist, J. Floß, I. Sh. Averbukh, J. W. Hepburn, and V. Milner, “Control of molecular rotation with a chiral train of ultrashort pulses,” *Phys. Rev. Lett.* **107**, 243004 (2011).
- [12] S. Zahedpour, J. K. Wahlstrand, and H. M. Milchberg, “Quantum control of molecular gas hydrodynamics,” *Phys. Rev. Lett.* **112**, 143601 (2014).
- [13] S. Zhdanovich, C. Bloomquist, J. Floß, I. Sh. Averbukh, J. W. Hepburn, and V. Milner, “Quantum resonances in selective rotational excitation of molecules with a sequence of ultrashort laser pulses,” *Phys. Rev. Lett.* **109**, 043003 (2012).
- [14] J. Floß, A. Kamalov, I. Sh. Averbukh, and P. H. Bucksbaum, “Observation of Bloch oscillations in molecular rotation,” *Phys. Rev. Lett.* **115**, 203002 (2015).
- [15] A. Kamalov, D. W. Broege, and P. H. Bucksbaum, “Dynamical localization in molecular alignment of kicked quantum rotors,” *Phys. Rev. A* **92**, 013409 (2015).
- [16] M. Bitter and V. Milner, “Rotational excitation of molecules with long sequences of intense femtosecond pulses,” submitted, arXiv:1509.05090 (2015).
- [17] C. W. Siders, J. L. W. Siders, A. J. Taylor, S.-G. Park, and A. M. Weiner, “Efficient high-energy pulse-train generation using a 2n-pulse Michelson interferometer,” *Appl. Opt.* **37**, 5302 (1998).
- [18] S. Zhou, D. Ouzounov, H. Li, I. Bazarov, B. Dunham, C. Sinclair, and F. W. Wise, “Efficient temporal shaping of ultrashort pulses with birefringent crystals,” *Appl. Opt.* **46**, 8488 (2007).
- [19] M. M. Wefers and K. A. Nelson, “Programmable phase and amplitude femtosecond pulse shaping,” *Opt. Lett.* **18**, 2032 (1993).
- [20] M. A. Dugan, J. X. Tull, and W. S. Warren, “High-resolution acousto-optic shaping of unamplified and amplified femtosecond laser pulses,” *J. Opt. Soc. Am. B.* **14**, 2348 (1997).
- [21] D. E. Leaird and A. M. Weiner, “Femtosecond optical packet generation by a direct space-to-time pulse shaper,” *Opt. Lett.* **24**, 853 (1999).
- [22] A. M. Weiner, S. Oudin, D. H. Reitze, and D. E. Leaird, “Shaping of femtosecond pulses using phase-only filters designed by simulated annealing,” *J. Opt. Soc. Am. A.*

- 10**, 1112 (1993).
- [23] A. Efimov, M. D. Moores, N. M. Beach, J. L. Krause, and D. H. Reitze, "Adaptive control of pulse phase in a chirped-pulse amplifier," *Opt. Lett.* **23**, 1915 (1998).
- [24] I. Pastirk, B. Resan, A. Fry, J. MacKay, and M. Dantus, "No loss spectral phase correction and arbitrary phase shaping of regeneratively amplified femtosecond pulses using MIIPS," *Opt. Express* **14**, 9537 (2006).
- [25] X. Liu, R. Wagner, A. Maksimchuk, E. Goodman, J. Workman, D. Umstadter, and A. Migus, "Nonlinear temporal diffraction and frequency shifts resulting from pulse shaping in chirped-pulse amplification systems," *Opt. Lett.* **20**, 1163 (1995).
- [26] A. Efimov and D. H. Reitze, "Programmable dispersion compensation and pulse shaping in a 26-fs chirped-pulse amplifier," *Opt. Lett.* **23**, 1612 (1998).
- [27] S. Zhou, F. W. Wise, and D. G. Ouzounov, "Divided-pulse amplification of ultrashort pulses," *Opt. Lett.* **32**, 871 (2007).
- [28] A. M. Weiner, "Femtosecond pulse shaping using spatial light modulators," *Rev. Sci. Instrum.* **71**, 1929 (2000).
- [29] The  $1/N$  scaling can be derived from the following consideration of a pulse train in the frequency domain. The spectrum of an infinite pulse train is a frequency comb. The separation of the comb teeth is inversely proportional to the train period  $T$ ,  $\Delta\omega \propto 1/T$ . The spectrum of a finite train of  $N$  pulses is the same comb convolved with the sinc function whose width is inversely proportional to  $NT$ ,  $\delta\omega \propto 1/(NT)$ . The ratio  $\delta\omega/\Delta\omega$  determines the amount of energy remaining in the train after shaping.